Stem Cell Research (2014) 12, 178–193

Available online at www.sciencedirect.com

ScienceDirect

www.elsevier.com/locate/scr

A complex interplay between PGC-1 co-activators and mTORC1 regulates hematopoietic recovery following 5-fluorouracil treatment

Sunanda Basu*

Department of Microbiology and Immunology, Indiana University School of Medicine, Indianapolis, USA

Received 14 June 2013; received in revised form 28 September 2013; accepted 15 October 2013
Available online 24 October 2013

Abstract In vitro stimulation of HSCs with growth factors generally leads to their depletion. Understanding the molecular mechanisms underlying expansion of HSCs in vivo following myeloablation could lead to successful expansion of HSCs ex vivo for therapeutic purposes. Current findings show that mTORC1 is activated in HSPCs following 5-fluorouracil treatment and that mTORC1 activation is dependent on mitochondrial ETC capacity of HSPCs. Moreover, expression of PGC-1 family members, proteins that regulate mitochondrial biogenesis, in HSPCs following 5-fluorouracil treatment changes; also, these proteins play a stage specific role in hematopoietic recovery. While PRC regulates HSCs' expansion during early recovery phase, PGC-1α regulates progenitor cell proliferation and recovery of hematopoiesis during later phase. During early recovery phase, PRC expression, mitochondrial activity and mTORC1 activation are relatively higher in PGC-1$\alpha^{-/-}$ HSCs compared to WT HSCs, and PGC-1$\alpha^{-/-}$ HSCs show greater expansion. Administration of rapamycin, but not NAC, during early recovery phase improves WT HSC numbers but decreases PGC-1$\alpha^{-/-}$ HSC numbers. The current findings demonstrate that mTOR activation can increase HSC numbers provided that the energy demand created by mTOR activation is successfully met. Thus, critical tuning between mTORC1 activation and mitochondrial ETC capacity is crucial for HSC maintenance/expansion in response to mitogenic stimulation.

Introduction

Expansion of hematopoietic stem cells (HSCs) in vitro using growth factors has been thwarted by findings that there is loss of HSCs during in vitro expansion. In steady-state hematopoiesis, a majority of HSCs remain quiescent; however, in response to 5-fluorouracil (5-FU) treatment, majority of HSCs undergo rapid proliferation and lead to hematopoietic recovery (Harrison and Lerner, 1991). Therefore, a better understanding of molecular pathways that regulate HSC expansion and recovery of hematopoiesis following 5-FU treatment may

Abbreviations: HSC, hematopoietic stem cell; HSPC, hematopoietic stem and progenitor cell; mTORC1, mammalian target of rapamycin complex1; ETC, electron transport chain; PGC-1α, peroxisome proliferator-activated receptor gamma co-activator-1α; PRC, PGC-1 related coactivator; NAC, N-acetyl cysteine.

* Indiana University School of Medicine, Research Institute No. 2 Bldg, Rm 302, 950 W Walnut Street, Indianapolis, IN 46202-5181, USA. Fax: +1 317 274 7592.
E-mail addresses: sbasu86@gmail.com, sunbasu@iupui.edu.

1873-5061
http://dx.doi.org/10.1016/j.scr.2013.10.006

allow us to develop protocols that will eventually lead to successful ex vivo expansion of HSCs.

Mammalian target of rapamycin (mTOR) kinase is the catalytic subunit of two complexes, mammalian target of rapamycin complex (mTORC) 1 and 2; mTORC1 and 2 have been respectively characterized as the rapamycin-sensitive and rapamycin-insensitive complexes (Laplante and Sabatini, 2009). Growth factors stimulate the mammalian target of rapamycin complex1 (mTORC1) pathway that controls cell growth and division (Fingar and Blenis, 2004). Activation of mTOR is regulated by adenosine triphosphate (ATP) levels in the cell (Dennis et al., 2001). Oxidative phosphorylation (OXPHOS), an oxygen dependent process that occurs in the mitochondria, is the major source of cellular ATP. Taken together, these findings raise the possibility that the interaction between the molecular pathways, mTOR activation and mitochondrial biogenesis, plays a deterministic role in ability of hematopoietic stem and progenitor cells (HSPCs) to successfully expand following 5-FU treatment. Mitochondria have their own DNA that encodes for 13 essential proteins of inner membrane respiratory apparatus but nuclear genes encode for a majority of respiratory proteins and all other gene products necessary for a variety of mitochondrial functions. The nucleo-mitochondrial interactions depend on regulation of transcription factors and peroxisome proliferator-activated receptor gamma co-activator (PGC-1) family of transcriptional co-activators that includes PGC-1α, PGC-1β and PGC-1 related coactivators (PRC) (Scarpulla, 2008). Although various PGC-1 family members can regulate mitochondrial biogenesis (Scarpulla, 2002; Uldry et al., 2006), PGC-1α is considered the master regulator of mitochondrial biogenesis (Puigserver and Spiegelman, 2003). PGC-1α is expressed in BM hematopoietic stem progenitor cells (HSPCs) (Basu et al., 2013).

While glycolysis is important for the maintenance of HSCs (Simsek et al., 2010; Takubo et al., 2010), the role of mitochondrial metabolism in hematopoiesis (Nakada et al., 2010; Gurumurthy et al., 2010), particularly in response to stress (Mortensen et al., 2011), is increasingly being realized. Indeed, recovery of peripheral blood cells (PBCs) following 5-FU treatment is significantly impaired in PGC-1α knockout (PGC-1$\alpha^{-/-}$) mice compared to wild type (WT) mice; however, steady-state hematopoiesis is not overtly affected in PGC-1$\alpha^{-/-}$ mice (Basu et al., 2013). Moreover, the impairment of PBC recovery is more profound in older PGC-1$\alpha^{-/-}$ mice (SB unpublished observation) consistent with age related degeneration of mitochondrial function (Pieri et al., 1993). These findings suggest a role of mitochondria in the recovery of hematopoiesis following 5-FU treatment.

To get an insight into mechanisms regulating HSC proliferation in vivo, recovery of hematopoiesis following 5-FU treatment in WT and PGC-1$\alpha^{-/-}$ mice was investigated in this study. The current study demonstrates that mitochondrial biogenesis is critical for HSPCs to optimally respond to mTORC1 activation and proliferate in response to mitogenic signals following 5-FU challenge. Moreover, the level of mTORC1 activation is regulated by the mitochondrial biogenesis potential of HSPCs. Interestingly, different members of the PGC-1 family play stage-specific roles in hematopoietic recovery following 5-FU treatment: while PRC is required for hematopoietic stem cell (HSC) proliferation during early recovery phase, PGC-1α is important for rapid proliferation of progenitors during late phase of hematopoietic recovery following 5-FU treatment.

Material and methods

Animal studies

All animal studies were evaluated and approved by the Institutional Animal Care and Use committee. PGC-1α knockout (PGC-1$\alpha^{-/-}$) mice were a kind gift from Prof. B. Spiegelman (DFCI, Boston, MA) and used after 9 backcrosses to C57/Bl6 mice. PGC-1$\alpha^{+/+}$ litter mate mice were used as a control and are designated as wild type (WT) in this study. C57/Bl6 mice were purchased from Jackson Laboratories; C57/Bl6:BoyJ F1 and Boy/J mice were from the In Vivo Core Therapeutic Facility of the Indiana University School of Medicine.

5-FU and rapamycin treatments

Mice were treated with 150 mg/kg wt of 5-FU intraperitoneally (i.p.) on day 0 and the changes in PBC counts and bone marrow (BM) cellularity was followed thereafter. Rapamycin (Sigma-Aldrich) was made in absolute ethanol at 10 mg/ml and further diluted in 5% Tween-80 (Sigma-Aldrich) and 5% PEG-400 (Hampton Research) (Chen et al., 2008). Rapamycin was delivered i.p. so that the measured dose of rapamycin (adjusted to mouse body weight) could be administered. Mice received 4 mg/kg rapamycin on days 1 and 3 or on day 8 post-5-FU treatment.

Phenotypic and functional analysis of BM cells

BM cells were obtained from the long bones (tibias and femurs) of mice. Lineage positive cells were identified based on staining pattern with fluorescent dye conjugated antibodies against B220, CD3, Gr-1, Mac-1, CD71 and Ter119 (BD Biosciences). The above set of antibodies, except CD71, was used to gate out the lineage positive cells for analysis of HSC/progenitor populations. For analysis of 5-FU treated BM on day 4 Mac-1 was not included in the lineage cocktail antibody for gating out lineage negative cells (Randall and Weissman, 1997). c-Kit$^+$Sca-1$^+$IL-7R$^-$Lin$^-$ cells are designated as KSL and c-kit$^+$IL-7R$^-$Lin$^-$ cells are designated as KL/MP. HSCs are defined as KSL IL-7R$^-$CD34$^-$, and MPPs defined as KSL IL-7R$^-$CD34$^+$. Since the expression of CD34 on HSCs alters following 5-FU treatment (Sato et al., 1999), I used SLAM marker in conjunction with KSL (Yilmaz et al., 2006) to enumerate changes in primitive and progenitor cell populations in the BM for up to 7 days following 5-FU treatment. The combination of SLAM markers used to identify progenitors differs between Yilmaz et al. (2006) and Wilson et al. (2008) and in this study the identification of the progenitors has been done as described by Yilmaz et al. (2006). Fluorochrome conjugated antibodies were purchased from eBioscience, Biolegend and BD Bioscience. Flow cytometry analysis was performed on an LSR II (BD Biosciences), and cells were sorted using FACSAria (BD Biosciences). Cell cycle status was determined by fixing and permeabilizing cells with BD Per/Fix buffer reagents (BD Pharmingen) and staining the cells with 2 μg/ml HOECHST 33342 (Invitrogen)

for 10 min followed by washing the cells and then staining with 4 μg/ml PyroninY. Mice were injected i.p. with BrdU (Sigma) at a dose of 0.1 mg/g body mass. BrdU uptake by BM cells was analyzed by staining the cells with anti-BrdU-APC staining kit (BD Pharmingen).

ROS, mitochondrial activity, ATP, NADH, and mTORC1 activation

Reactive oxygen species (ROS) and mitochondrial activity in various BM sub-populations were measured using the fluorescent dyes 2′,7′-dichlorofluorescein diacetate DCFDA (Invitrogen) and MitoTracker Deep Red (MDR) (Invitrogen), respectively as previously described (Basu et al., 2013). Mitochondrial transmembrane potential ($\Delta\psi_m$) was assessed in live cells by staining with JC-1 dye as described earlier (Basu et al., 2013; Cossarizza and Salvioli, 2001). ATP content was measured using Cell-Titer-Glo luminescent cell viability kit (Promega) as described previously (Basu et al., 2013). Endogenous NADH fluorescence was measured using flow cytometrically using a UV laser (LSR II, BD Biosciences) (Chance and Thorell, 1959). For measuring mTORC1 activation, BM cells were fixed using 1.5% paraformaldehyde, permeabilized using cold acetone as described previously (Kalaitzidis and Neel, 2008) and then stained with Alexa-488 conjugated phosphorylated S6 ribosomal protein (pS6) or control antibody (Cell Signaling). The samples were analyzed using flow cytometry using FlowJo software. As a measure of mTORC1 activation, the level of phosphorylated p70S6kinase (Thr389) (pp70S6K) was measured using western blot, in addition to pS6.

Western blot

Lineage negative cells were sorted based on staining pattern of BM cells with fluorescent dye conjugated antibodies against B220, CD3, Gr-1, Mac-1, and Ter119 (Mac-1 antibody was not included in the antibody cocktail for sorting of day 4 post-5-FU BM cells). Cells were lysed and were electrophoresed on 4–12% Tris-glycine gel (Invitrogen) and then blotted onto a polyvinyl difluoride (PVDF) membrane (Basu and Broxmeyer, 2005). The membrane was probed with different antibodies: pp53 (ser15), p53, pACC (ser79), pAMPK-α (Thr172), AMPKα, pp90RSK (Thr359/Ser363), pp70S6K (Thr389) (Cell Signaling) and β-actin (Sigma). Between probing with each antibody the blot was stripped using stripping buffer and thereafter washed 3 times with wash buffer.

Gene expression by qRT-PCR

mRNA was isolated and cDNA prepared using MACS cDNA module (Miltenyi Biotec) from freshly sorted cells. Expression of genes was studied using real-time polymerase chain reaction (PCR; Stratagene, Mx3000P) based on SYBR Green (Invitrogen) monitoring of PCR product accumulation. PCR primer pairs were purchased from SABioscience.

Bone marrow transplantation

The recipient mice were fed with doxyrubicin for a week before irradiation (950 rad) and continued on the

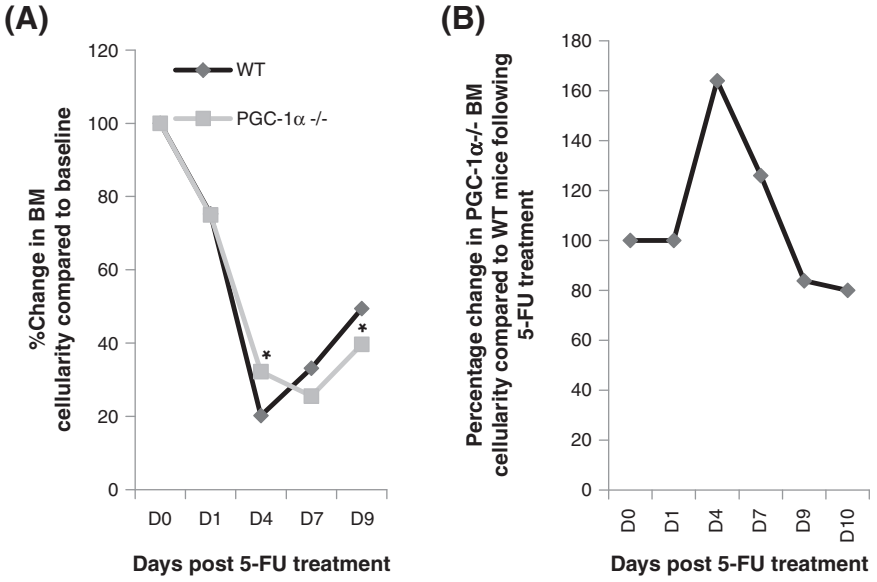

Figure 1 Kinetics of changes in peripheral blood cell count and bone marrow cellularity following 5-FU challenge. Kinetic of changes in peripheral blood cell count following 5-FU challenge in (Ai) young (8–10 wk) and (Aii) old (>20 wk) WT and PGC-1$\alpha^{-/-}$ mice (n = 4–5 mice per genotype, *p < 0.02 compared to WT mice). (Bi) Percentage change in BM cellularity of WT and PGC-1$\alpha^{-/-}$ mice compared to basal level and (Bii) change in PGC-1$\alpha^{-/-}$ BM cellularity compared to WT mice following 5-FU treatment (n = 3–5 mice per time point; *p < 0.05 compared to WT mice).

doxyrubicin supplemented feed for the next 2 months to prevent spontaneous infection. Competitive repopulation assays were performed as previously described. Briefly, either 2×10^5 (1:1 group) or 0.5×10^5 (0.25:1 group) BM cells from either PGC-1$\alpha^{-/-}$ mice or C57/Bl6 mice (CD45.2) were mixed with 2×10^5 BM cells from BoyJ (CD45.1) mice and injected into irradiated recipient C57/Bl6:BoyJ F1double-positive recipients (CD45.1:CD45.2). PB was obtained from the tail veins of recipients at indicated times to monitor chimerism. RBCs were lysed by RBC lysis buffer (ammonium chloride/potassium bicarbonate buffer) before staining. For secondary transplant, BM cells from each of the primary recipient were injected into three irradiated (950 rad) secondary recipients (2×10^6 cells/secondary recipient mouse). Chimerism in PB was evaluated 2 months after transplantation.

Statistical analysis

Data is presented as mean ± SD unless indicated otherwise. Significance of differences was analyzed using Student's 2-tailed *t*-test.

Results

Loss of PGC-1α has a differential effect on early and late phase of hematopoietic recovery following 5-FU treatment

5-FU treatment kills proliferating progenitors but spares the HSCs (Lerner and Harrison, 1990). Proliferation of HSCs and progenitors in the BM precedes recovery of PBC count following 5-FU treatment (Harrison and Lerner, 1991). Indeed, 5-FU treatment led to reduction in BM cellularity in both WT and PGC-1$\alpha^{-/-}$ mice (Fig. 1A). BM cellularity was lower in PGC-1$\alpha^{-/-}$ than in WT mice on days 9 and 10 (Fig. 1B), surprisingly, on day 4, BM cellularity was significantly higher in PGC-1$\alpha^{-/-}$ than in WT mice (Figs. 1A–B). Recovery of BM hematopoiesis following 5-FU treatment occurs broadly in two phases. In the first phase (from days 2 to 5), HSCs are stimulated to proliferate rapidly to replenish the progenitor cell pool; however, very little progenitor expansion occurs during this period, and both BM cellularity and PBC counts reach nadir (Harrison and Lerner, 1991; Randall and Weissman, 1997; Jansen et al., 1991). In the second phase, proliferation of HSCs returns to near normal level, but MPs proliferate rapidly followed by an overshoot of BM and PBC counts, which eventually return to normal level. Therefore, to understand why recovery of PBC counts in PGC-1$\alpha^{-/-}$ mice is compromised, I examined these two phases of recovery, which will hereafter be referred to as early and late phases of hematopoietic recovery in PGC-1$\alpha^{-/-}$ and WT mice following 5-FU treatment.

Early phase of hematopoietic recovery—Increased HSC and MP pools in BM of PGC-1$\alpha^{-/-}$ mice following 5-FU treatment

On day 4 post-5-FU both BM cellularity and PBC count were higher in PGC-1$\alpha^{-/-}$ than in WT mice (Fig. 2Ai–ii). Also, both the proportions and total numbers of MP and HSC were higher in PGC-1$\alpha^{-/-}$ than in WT mice on day 4 (Fig. 2Bi–iii). The difference in progenitor and HSC numbers in PGC-1$\alpha^{-/-}$ from those in WT mice on day 4 was not due to a difference in susceptibility of WT and PGC-1$\alpha^{-/-}$ BM cells to the killing effect of 5-FU as the reduction in PBC count, total BM cellularity, composition of early and mature BM cells, cell cycle status, and apoptotic BM cells were comparable between PGC-1$\alpha^{-/-}$ and WT mice on day 1 post-5-FU treatment (Fig. S1Ai–v, B & Ci–ii). Therefore, the larger HSPC pool on day 4 in PGC-1$\alpha^{-/-}$ mice was likely due to a greater proliferation of PGC-1$\alpha^{-/-}$ HSPCs. To investigate this possibility, bromodeoxyuridine (BrdU) was injected into the mice on day 3 post-5-FU treatment. Examination of BM cells 24 h post-BrdU injection revealed that a significantly greater proportion of MPs (identified as IL-7R$^-$KL) and HSC enriched fraction (IL-7R$^-$KSL) of BM cells were proliferating in PGC-1$\alpha^{-/-}$ compared to WT mice. These cells were also cycling faster in PGC-1$\alpha^{-/-}$ mice since a greater proportion of these cells in the G0/G1 phase were BrdU positive (Fig. 2Ci–iii) in these mice. Moreover, significantly lower proportions of IL-7R$^-$KSL cells and MPs underwent apoptosis as demonstrated by the comparatively lower proportion of cells in the subG0 fraction in PGC-1$\alpha^{-/-}$ compared to WT mice (Fig. 2Ci–iii). Thus, enhanced proliferative potential coupled with lower apoptosis of HSCs and MPs in PGC-1$\alpha^{-/-}$ mice compared to WT mice during the early recovery phase results in increased HSC and MP pools in these mice.

HSCs are spared by a single dose of 5-FU; however, a second dose of 5-FU, administered 4 days after the primary dose, kills a significant number of HSCs (Harrison and Lerner, 1991). Indeed, total numbers of both MPs and HSCs (Fig. 2Di–iv) were significantly reduced in both WT and PGC-1$\alpha^{-/-}$ mice following (next day) two doses of 5-FU, administered on days 0 and 4. Interestingly, total numbers of HSCs and MPs were higher in PGC-1$\alpha^{-/-}$ compared to WT mice after 2 doses of 5-FU (Fig. 2Diii–iv). 5-FU kills actively cycling cells and significantly greater proportions of MPs and HSCs were found to be actively cycling following a single dose of 5-FU in PGC-1$\alpha^{-/-}$ mice. This finding suggested that PGC-1$\alpha^{-/-}$ HSCs have enhanced proliferative potential following 5-FU treatment, enabling them to regenerate more HSCs. Indeed, a greater proportion of PGC-1$\alpha^{-/-}$ HSCs compared to WT were in cell cycle following 2 doses of 5-FU treatment (Fig. S2).

Despite an increase in phenotypically defined HSC and MP pools in PGC-1$\alpha^{-/-}$ mice during early recovery phase, attenuated recovery of blood cells in PGC-1$\alpha^{-/-}$ compared to WT mice following 5-FU treatment raised questions about the functional status of phenotypically identified PGC-1$\alpha^{-/-}$ HSC population. To address this issue, BM cells of 5-FU treated WT and PGC-1$\alpha^{-/-}$ mice were used in competitive repopulation assay using BM cells from BoyJ mice as the competitor cells. PGC-1$\alpha^{-/-}$ BM cells harvested 6 days post-5-FU treatment had greater competitive re-populating activity than similarly treated WT BM cells (39.6 ± 16% vs 2.5 ± 2.2% PGC-1$\alpha^{-/-}$ vs WT cells, respectively, in PB of recipient mice at 4 months post-transplantation; at 0.25:1 donor: competitor ratio, 5×10^4 donor cells in a graft). This difference in repopulating activity is not due to a difference in homing ability of WT and PGC-1$\alpha^{-/-}$ BM cells as indicated by a similar proportion of WT and PGC-1$\alpha^{-/-}$ BM cells in recipient mice BM on day 8 (Figs. S3A–C), although donor cell contribution in recipient mice was different 14 days post-transplantation.

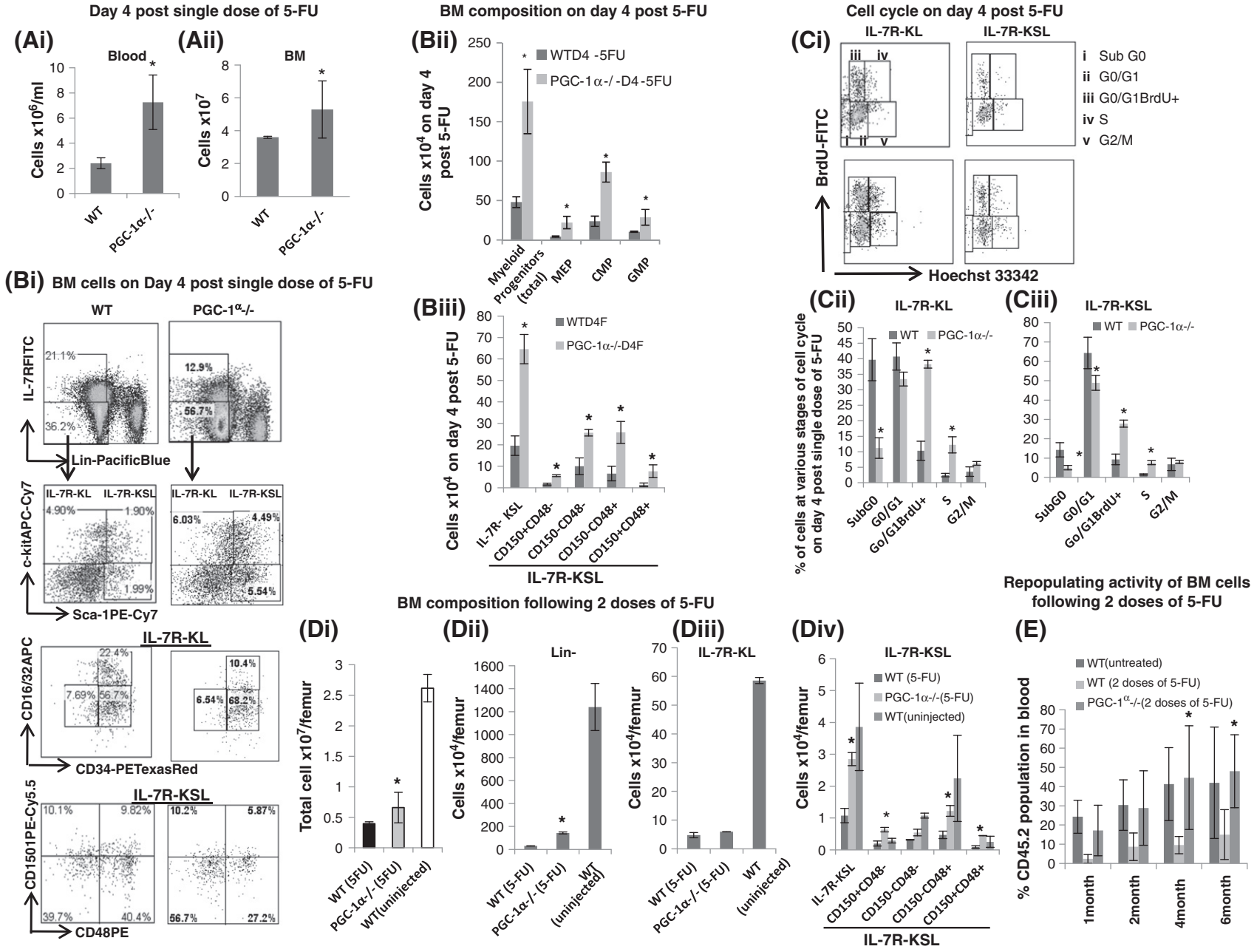
Day 4 post single dose of 5-FU
(Ai)
Blood
Cells x10^6/ml
WT
PGC-1α-/-
(Aii)
BM
Cells x10^7
WT
PGC-1α-/-
BM composition on day 4 post 5-FU
(Bii)
WTD4 -5FU
PGC-1α-/-D4-5FU
Cells x10^4 on day 4 post 5-FU
Myeloid Progenitors (total)
MEP
CMP
GMP
(Bi) BM cells on Day 4 post single dose of 5-FU
WT
PGC-1α-/-
IL-7RFITC
21.1%
36.2%
12.9%
56.7%
Lin-PacificBlue
IL-7R-KL
IL-7R-KSL
4.90%
1.90%
1.99%
6.03%
4.49%
5.54%
c-kitAPC-Cy7
Sca-1PE-Cy7
IL-7R-KL
CD16/32APC
22.4%
7.69%
56.7%
10.4%
6.54%
68.2%
CD34-PETexasRed
IL-7R-KSL
CD1501PE-Cy5.5
10.1%
9.82%
39.7%
40.4%
10.2%
5.87%
56.7%
27.2%
CD48PE
(Biii)
WTD4F
PGC-1α-/-D4F
Cells x10^4 on day 4 post 5-FU
IL-7R- KSL
CD150+CD48-
CD150-CD48-
CD150-CD48+
CD150+CD48+
IL-7R-KSL
Cell cycle on day 4 post 5-FU
(Ci)
IL-7R-KL
IL-7R-KSL
i Sub G0
ii G0/G1
iii G0/G1BrdU+
iv S
v G2/M
BrdU-FITC
Hoechst 33342
(Cii)
IL-7R-KL
WT
PGC-1α-/-
% of cells at various stages of cell cycle on day 4 post single dose of 5-FU
SubG0
G0/G1
Go/G1BrdU+
S
G2/M
(Ciii)
IL-7R-KSL
WT
PGC-1α-/-
SubG0
G0/G1
Go/G1BrdU+
S
G2/M
BM composition following 2 doses of 5-FU
(Di)
Total cell x10^7/femur
WT (5FU)
PGC-1α-/-(5FU)
WT(uninjected)
(Dii)
Lin-
Cells x10^4/femur
WT (5-FU)
PGC-1α-/-(5-FU)
WT (uninjected)
(Diii)
IL-7R-KL
Cells x10^4/femur
WT (5-FU)
PGC-1α-/-(5-FU)
WT (uninjected)
(Div)
IL-7R-KSL
WT (5-FU)
PGC-1α-/-(5-FU)
WT(uninjected)
Cells x10^4/femur
IL-7R-KSL
CD150+CD48-
CD150-CD48-
CD150-CD48+
CD150+CD48+
IL-7R-KSL
Repopulating activity of BM cells following 2 doses of 5-FU
(E)
WT(untreated)
WT (2 doses of 5-FU)
PGC-1α-/-(2 doses of 5-FU)
% CD45.2 population in blood
1month
2month
4month
6month

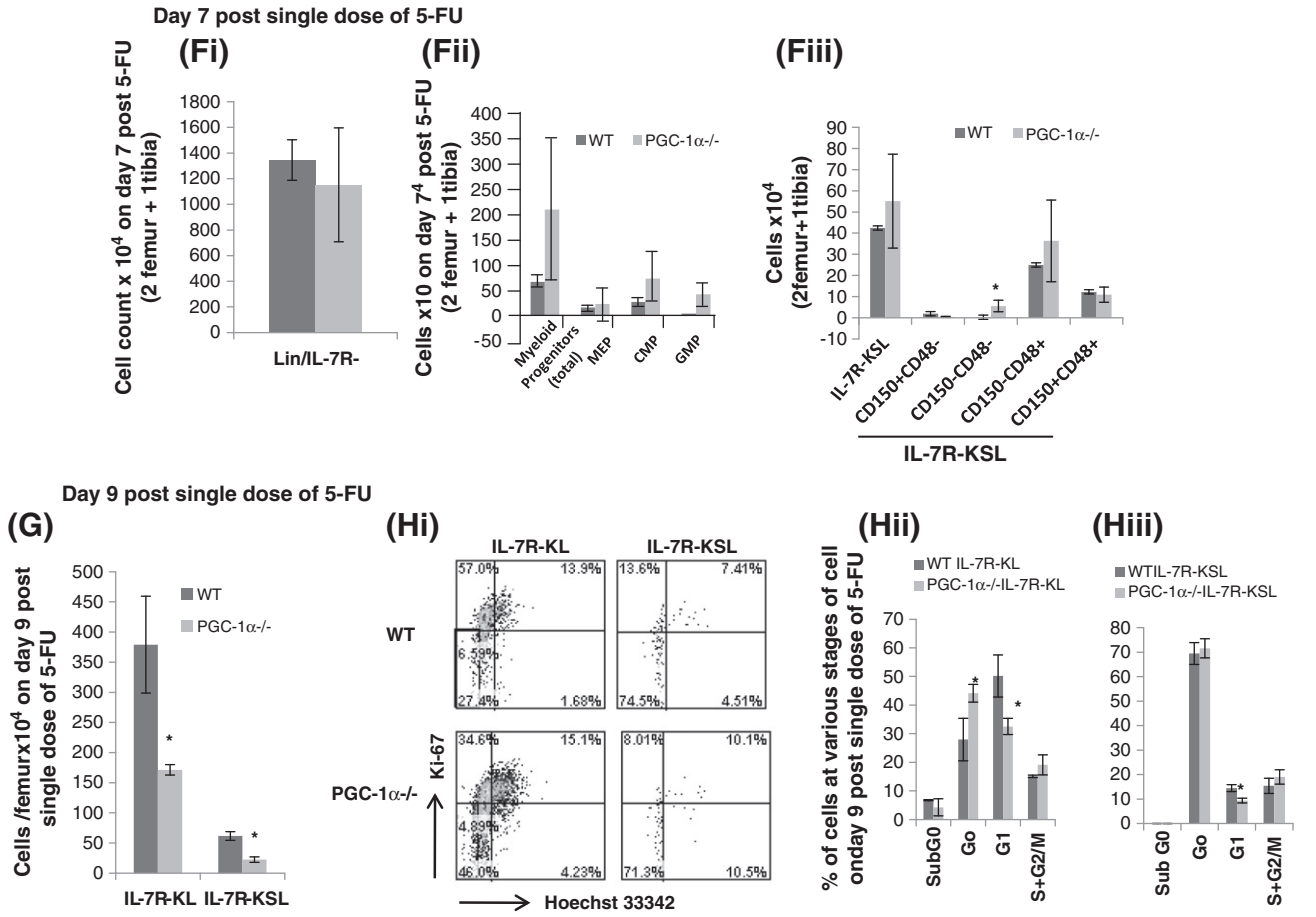

Figure 2 HSC and progenitor cell numbers in the BM during early and late recovery phases of hematopoiesis following 5-FU challenge. (Ai) PBC and (Aii) total BM cell (2 femurs and 1 tibia) counts on day 4 post-5-FU challenge. (Bi) Representative dot plot showing changes in HSCs and progenitor cells on day 4. (Bii) Total numbers of HSCs, multipotential progenitors and (Bii) MPs in BM (2 tibias and 1 femur) on day 4 (n = 3–5; *p < 0.05). (Ci) Mice were treated with 5-FU (150 mg/kg wt) and injected with BrdU (i.p.) 3 days later. 24 h post-BrdU injection, BM cells were harvested and stained with fluorochrome conjugated antibodies against specific surface markers and BrdU as detailed in Materials and methods. Representative dot blot showing cell cycle status of HSC enriched fraction and progenitor cells on day 4. Proportion of (Cii) MPs (IL-7R$^-$KL) and (Ciii) HSC enriched (IL-7R$^-$KSL) BM cells in undergoing proliferation and apoptosis in WT and PGC-1$\alpha^{-/-}$ mice on day 4 are shown (n = 3; *p < 0.05, compared to WT mice). (Di) BM cellularity, (Dii) lineage negative, (Diii) MPs, (Div) and HSCs of WT and PGC-1$\alpha^{-/-}$ mice following two doses of 5-FU administered 4 days apart and those of untreated WT mice are shown (n = 3; *p < 0.05). (E) Comparison of repopulating activity of BM cells of WT and PGC-1$\alpha^{-/-}$ mice harvested on day 6 following 2 doses of 5-FU treatment, administered 3 days apart (days 0 and 4), and BM cells from untreated WT mice is shown (n = 5 recipient mice in each group; * p < 0.05 compared to WT mice treated with 2 doses of 5-FU). (Fi–iii) Total number of lineage negative cells, MPs as well as HSCs cells (in 2 tibias + 1 femur is shown) is shown on day 7 (n = 3; p < 0.05 compared to WT mice). (G) Total MPs and HSC enriched population (IL-7R$^-$KSL) on day 9 post-5-FU challenge are shown. (Hi) BM cells were stained with a panel of fluorochrome conjugated phenotype defining specific antibodies and then fixed and stained with Hoechst and anti-Ki-67 antibody. Cell cycle status of MPs and HSC enriched fraction (IL-7R$^-$KSL) on day 7 was determined by FACS analysis. Proportions of (Hii) MPs and (Hiii) HSC enriched fraction of cells at the various stages of cell cycle on day 7 are shown (n = 3; p < 0.05 compared to WT mice).

Furthermore, consistent with previous reports, competitive repopulating potential of WT and PGC-1$\alpha^{-/-}$ BM cells were significantly reduced when 2 doses of 5-FU were administered 5 days apart (contribution of donor derived cells in peripheral blood of recipient mice at 0.25:1 donor competitor cell ratio: 0.25 ± 0.3 (WT) and 2.5 ± 2.8% (PGC-1$\alpha^{-/-}$) after doses of 5-FU compared to 2.5 ± 2.2 (WT) versus 39.6 ± 16% (PGC-1$\alpha^{-/-}$) after 1 dose of 5-FU, at 4 months). However, relative repopulating activity of PGC-1$\alpha^{-/-}$ BM cells was higher than WT BM cells as observed in response to single dose of 5-FU (Fig. 2E). This finding confirmed that there is a greater expansion of long term-repopulating cells in PGC-1$\alpha^{-/-}$ mice compared to WT mice following 5-FU treatment.

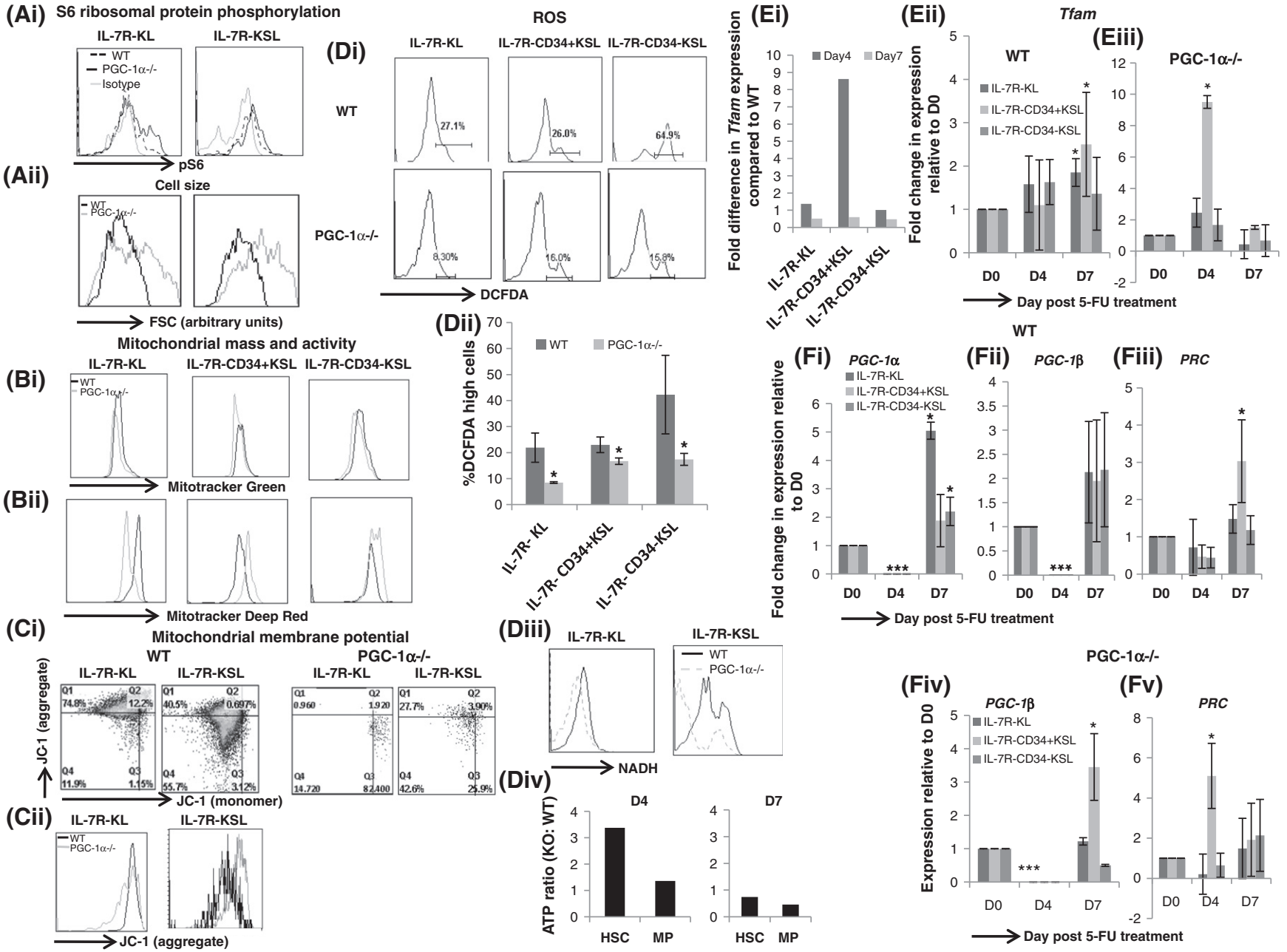
(Ai) S6 ribosomal protein phosphorylation
IL-7R-KL
IL-7R-KSL
WT
PGC-1α-/-
Isotype
pS6
(Aii)
Cell size
WT
PGC-1α-/-
FSC (arbitrary units)
(Di)
ROS
IL-7R-KL
IL-7R-CD34+KSL
IL-7R-CD34-KSL
WT
PGC-1α-/-
27.1%
26.0%
64.9%
8.30%
16.0%
15.8%
DCFDA
(Ei)
Fold difference in Tfam expression compared to WT
Day4
Day7
IL-7R-KL
IL-7R-CD34+KSL
IL-7R-CD34-KSL
(Eii)
Tfam
WT
PGC-1α-/-
IL-7R-KL
IL-7R-CD34+KSL
IL-7R-CD34-KSL
Fold change in expression relative to D0
D0
D4
D7
Day post 5-FU treatment
(Eiii)
Mitochondrial mass and activity
(Bi)
IL-7R-KL
IL-7R-CD34+KSL
IL-7R-CD34-KSL
WT
PGC-1α-/-
Mitotracker Green
(Bii)
Mitotracker Deep Red
(Dii)
%DCFDA high cells
WT
PGC-1α-/-
IL-7R- KL
IL-7R- CD34+KSL
IL-7R- CD34-KSL
(Fi)
PGC-1α
(Fii)
PGC-1β
(Fiii)
PRC
WT
IL-7R-KL
IL-7R-CD34+KSL
IL-7R-CD34-KSL
Fold change in expression relative to D0
***
D0
D4
D7
Day post 5-FU treatment
(Ci)
Mitochondrial membrane potential
WT
PGC-1α-/-
IL-7R-KL
IL-7R-KSL
JC-1 (aggregate)
JC-1 (monomer)
Q1 74.8% Q2 12.2% Q4 11.9% Q3 1.15%
Q1 40.5% Q2 0.697% Q4 55.7% Q3 3.12%
Q1 0.960 Q2 1.920 Q4 14.720 Q3 82.400
Q1 27.7% Q2 3.90% Q4 42.6% Q3 25.9%
(Cii)
IL-7R-KL
IL-7R-KSL
WT
PGC-1α-/-
JC-1 (aggregate)
(Diii)
IL-7R-KL
IL-7R-KSL
WT
PGC-1α-/-
NADH
(Div)
ATP ratio (KO: WT)
D4
D7
HSC
MP
(Fiv)
PGC-1β
(Fv)
PRC
PGC-1α-/-
IL-7R-KL
IL-7R-CD34+KSL
IL-7R-CD34-KSL
Expression relative to D0
***
D0
D4
D7
Day post 5-FU treatment

Late phase of hematopoietic recovery—Proliferation of MPs is compromised in PGC-1$\alpha^{-/-}$ mice

Impaired recovery of PBCs following 5-FU treatment in PGC-1$\alpha^{-/-}$ mice, despite higher proliferative potential and a larger pool of HSCs during early phase, suggested that proliferative capacity of hematopoietic progenitors during second phase is impaired in PGC-1$\alpha^{-/-}$ mice. Indeed, the differences between WT and PGC-1$\alpha^{-/-}$ mice in total BM cellularity and in HSPC pool observed on day 4 narrowed on day 7 (Figs. 1A–B & 2Fi–iii), and this was followed by a reversal of the trend in BM cellularity and composition on day 9 (Figs. 1A–B & 2G). There were fewer HSCs on day 7 in PGC-1$\alpha^{-/-}$ compared to WT mice and both the total number of BM cells, MPs and IL-7R^{-}KSL cells were lower in PGC-1$\alpha^{-/-}$ compared to WT mice (Fig. 2G) on day 9. Moreover, the proliferative potential of the MPs was impaired in PGC-1$\alpha^{-/-}$ mice (Fig. 2Hi–iii). These findings demonstrate that the defect in the later recovery phase underlies the impaired recovery of blood cells in PGC-1$\alpha^{-/-}$ mice following 5-FU treatment.

Analysis of mTORC1 activation, PGC-1 family members' expression, and mitochondrial metabolism following 5-FU treatment

Early phase of hematopoietic recovery

Cytokine-stimulated mTORC1 signaling plays an important role in cell growth and division (Sengupta et al., 2010). To gain insight into the molecular mechanism underlying the differences in proliferative potential of WT and PGC-1$\alpha^{-/-}$ HSPCs post-5-FU treatment, I therefore, evaluated mTORC1 activation level in WT and PGC-1$\alpha^{-/-}$ HSPCs. Basal mTORC1 activation levels of WT and PGC-1$\alpha^{-/-}$ BM cells, as measured by pS6 level, were comparable (Fig. S4). However, on day 4, pS6 level was higher in PGC-1$\alpha^{-/-}$ HSPCs compared to WT (Fig. 3Ai). Moreover, pp70S6k (Thr389) was also higher in PGC-1$\alpha^{-/-}$ HSPCs compared to WT; however, no difference in phosphorylation state of p90RSK was observed (Fig. S5) thus demonstrating that mTORC1 activity was higher in PGC-1$\alpha^{-/-}$ HSPCs compared to WT on day 4. Moreover, PGC-1$\alpha^{-/-}$ HSPCs were larger in size compared to WT HSPCs (Fig. 3Aii), consistent with higher mTORC1 activation (Fingar and Blenis, 2004). Activation of mTORC1 leads to biosynthetic processes, increasing demand for energy. Therefore, it is conceivable that activation of mTORC1 would lead to increased mitochondrial metabolism to meet the increased demand for ATP. On day 4, mitochondrial masses of PGC-1$\alpha^{-/-}$ and WT HSPCs were comparable (Fig. 3Bi); however, a greater proportion of WT MPs (IL-7R^{-}KL) had higher mitochondrial activity, indicated by MitoTracker Deep Red (MDR) fluorescence intensity and mitochondrial transmembrane potential ($\Delta\psi_m$) (JC-1$_{aggregate}$ MFI) (Figs. 3Bii & Ci–ii). Interestingly, the proportion of IL-7R^{-}KSL cells with actively respiring mitochondria was higher in PGC-1$\alpha^{-/-}$ compared to WT mice, demonstrated by MDR and JC-1 staining (proportion of cells expressing JC-1$_{aggregate}$) (Figs. 3Bii & Ci). JC-1 is a protonic dye, meaning its accumulation inside the mitochondria is dependent on the polarized state of mitochondria. JC-1$_{aggregate}$ formation causes a shift from green to red fluorescence emission with increasing concentration of the dye accumulation (i.e., aggregation) in the mitochondria instead of fluorescence quenching (Smiley et al., 1991). Therefore, the fluorescence intensity of the JC-1 aggregate is an indication of the mitochondrial membrane potential in the cell. In addition to high $\Delta\psi_m$, intracellular reactive oxygen species (ROS) and NADH levels were also higher in WT MPs and HSC enriched fraction of BM cells (Fig. 3Di–iii), but relative ATP level was lower (Fig. 3Div), suggesting that WT HSPCs had aberrant mitochondrial functions on day 4. Although stimulation with growth factors increases mitochondrial metabolism and $\Delta\psi_m$, a dramatic increase in $\Delta\psi_m$ makes the cells susceptible to apoptosis (Banki et al., 1999). Thus, higher $\Delta\psi_m$ and aberrant mitochondrial function and lower ATP content of WT HSPCs (Figs. 3Ci, Di–iv & Fig. S6) explain, at least in part, WT HSPCs' lower proliferative potential and higher apoptosis on day 4 post-5-FU treatment.

Comparative differences in $\Delta\psi_m$, ATP, intracellular NADH and ROS levels between WT and PGC-1$\alpha^{-/-}$ HSPCs suggested that there are differences in respiratory chain capacity between WT and PGC-1$\alpha^{-/-}$ HSPCs, which could explain the defects in OXPHOS, and thus energy producing capacity, of WT HSPCs. Regulation of respiratory chain capacity depends both on the nuclear and mitochondrial genomes (Scarpulla, 2008; Scarpulla, 2002). *Tfam* is essential for mtDNA transcription; loss of *Tfam* causes depletion of mtDNA, severe respiratory chain deficiency, loss of mitochondrial transcripts and of mtDNA-encoded polypeptides (Larsson et al., 1998). Although at baseline *Tfam* expressions are comparable in WT and PGC-1$\alpha^{-/-}$ HSPC (Fig. S7A), on day 4, *Tfam* levels were lower in WT compared to corresponding PGC-1$\alpha^{-/-}$ HSPCs

Figure 3 mTORC1 activation and mitochondrial activity during early recovery phase following 5-FU challenge. Representative plot of (A) phospho-S6 level and (Aii) cell size as measured using flow cytometry on day 4 post-5-FU of MPs and HSC enriched fraction (IL-7R^{-}KSL) of BM cells of WT and PGC-1$\alpha^{-/-}$ mice are shown (n = 3–5 mice). Representative plot showing (Bi) mitochondrial mass and (Bii) mitochondrial activity of various sub-populations of BM cells on day 4 (n = 3 mice). (Ci) Representative plot of JC-1 staining pattern, as a measure of $\Delta\psi_m$, of various fractions of BM cells and (Cii) the average intensity of JC-1 aggregate fluorescence of MPs (IL-7R^{-}KL) and IL-7R^{-}KSL cells of WT and PGC-1$\alpha^{-/-}$ mice on day 4 are shown (n = 3). (Di) Representative plot showing DCFDA staining pattern, as a measure of intracellular ROS level and (Dii) quantitative analysis of ROS level in various fractions of BM cells of WT and PGC-1$\alpha^{-/-}$ mice on day 4 are shown (n = 3, *$p < 0.05$). (Diii) Representative plot indicating intracellular NADH level in WT and PGC-1$\alpha^{-/-}$ sub-population of BM cells on day 4 post-5-FU challenge. (Div) Ratio of ATP in WT and PGC-1$\alpha^{-/-}$ BM subpopulations on day 4 and day 7 post-5-FU challenge (n = 3 mice in each experiment). (Ei) Changes in *Tfam* expression in PGC-1$\alpha^{-/-}$ compared to WT BM cells and *Tfam* expression pre- and post-5-FU treatment in (Ei) WT and (Eii) PGC-1$\alpha^{-/-}$ mice. (Fi–v) Expression of *PGC-1α*, *PGC-1β* and *PRC* on day 0 and various days post-5-FU treatment in WT and PGC-1$\alpha^{-/-}$ mice. *** Not detectable. Data shown is the mean of 2–3 experiments and in each experiment 3 mice of each genotype for each time point were analyzed (*$p < 0.05$ compared to basal value).

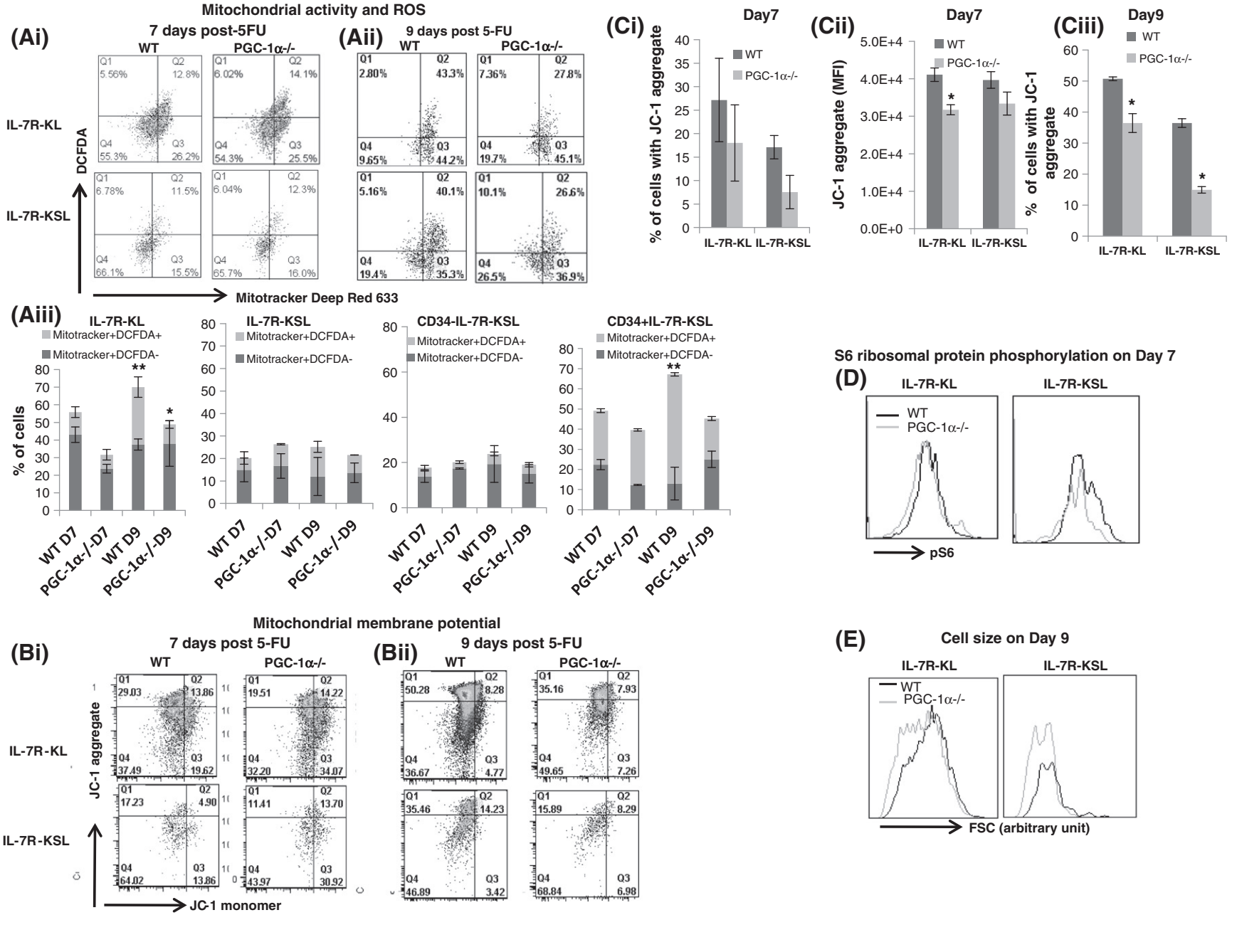
Mitochondrial activity and ROS
(Ai)
7 days post-5FU
WT
PGC-1α-/-
IL-7R-KL
IL-7R-KSL
DCFDA
Mitotracker Deep Red 633
Q1 5.56% Q2 12.8% Q4 55.3% Q3 26.2%
Q1 6.02% Q2 14.1% Q4 54.3% Q3 25.5%
Q1 6.78% Q2 11.5% Q4 66.1% Q3 15.5%
Q1 6.04% Q2 12.3% Q4 65.7% Q3 16.0%
(Aii)
9 days post 5-FU
WT
PGC-1α-/-
Q1 2.80% Q2 43.3% Q4 9.65% Q3 44.2%
Q1 7.36% Q2 27.8% Q4 19.7% Q3 45.1%
Q1 5.16% Q2 40.1% Q4 19.4% Q3 35.3%
Q1 10.1% Q2 26.6% Q4 26.5% Q3 36.9%
(Ci)
Day7
% of cells with JC-1 aggregate
WT
PGC-1α-/-
IL-7R-KL
IL-7R-KSL
(Cii)
Day7
JC-1 aggregate (MFI)
WT
PGC-1α-/-
IL-7R-KL
IL-7R-KSL
(Ciii)
Day9
% of cells with JC-1 aggregate
WT
PGC-1α-/-
IL-7R-KL
IL-7R-KSL
(Aiii)
IL-7R-KL
IL-7R-KSL
CD34-IL-7R-KSL
CD34+IL-7R-KSL
Mitotracker+DCFDA+
Mitotracker+DCFDA-
% of cells
WT D7
PGC-1α-/-D7
WT D9
PGC-1α-/-D9
S6 ribosomal protein phosphorylation on Day 7
(D)
IL-7R-KL
IL-7R-KSL
WT
PGC-1α-/-
pS6
Mitochondrial membrane potential
(Bi)
7 days post 5-FU
WT
PGC-1α-/-
IL-7R-KL
IL-7R-KSL
JC-1 aggregate
JC-1 monomer
Q1 29.03 Q2 13.86 Q4 37.49 Q3 19.62
Q1 19.51 Q2 14.22 Q4 32.20 Q3 34.07
Q1 17.23 Q2 4.90 Q4 64.02 Q3 13.86
Q1 11.41 Q2 13.70 Q4 43.97 Q3 30.92
(Bii)
9 days post 5-FU
WT
PGC-1α-/-
Q1 50.28 Q2 8.28 Q4 36.67 Q3 4.77
Q1 35.16 Q2 7.93 Q4 49.65 Q3 7.26
Q1 35.46 Q2 14.23 Q4 46.89 Q3 3.42
Q1 15.89 Q2 8.29 Q4 68.84 Q3 6.98
(E)
Cell size on Day 9
IL-7R-KL
IL-7R-KSL
WT
PGC-1α-/-
FSC (arbitrary unit)

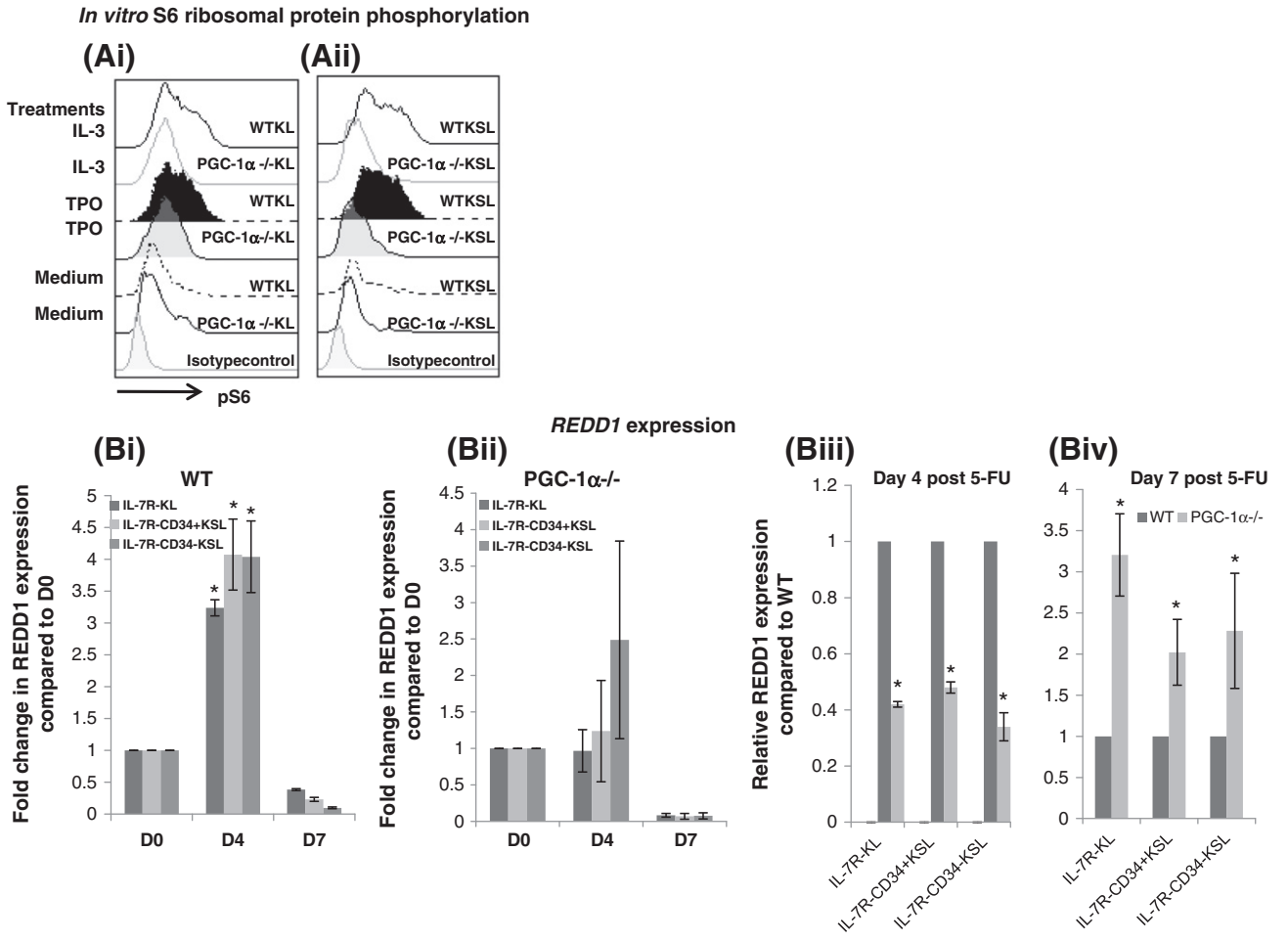

Figure 5 mTORC1 activation in vitro by growth factors stimulation and *REDD1* level in BM cells following 5-FU challenge. (A) Freshly isolated BM cells stimulated with thrombopoietin (TPO, 100 ng/ml) or interleukin-3 (IL-3, 50 ng/ml) or cultured in medium alone for 20 min and then they were washed and fixed. Cells were thereafter stained with antibodies against specific surface markers and pS6 or isotype matched antibody. Representative plot of pS6 level in different BM sub-populations is shown (n = 3). (Bi–ii) Fold change in *REDD1* expression in WT and PGC-1$\alpha^{-/-}$ BM sub-populations after 5-FU treatment relative to baseline expression. REDD1 expression in various sub-populations of PGC-1$\alpha^{-/-}$ BM cells relative to expression in WT BM cells on (Biii) day 4 and (Biv) day 7 post-5-FU treatment (n = 3, *$p < 0.05$).

(Fig. 3Ei–iii). PGC-1 family of co activators regulates *Tfam* expression (Scarpulla, 2008; Kelly and Scarpulla, 2004). Although HSPCs express all members of PGC-1 family at steady-state (Basu et al., 2013) *PGC-1α* and *PGC-1β* expressions were not detectable and only *PRC* expression was detectable in HSPCs (Fig. 3Fi–v) on day 4 post-5-FU treatment. Importantly, expression of PRC on day 4 was significantly higher in PGC-1$\alpha^{-/-}$ compared to WT HSPCs (Fig. S7B), particularly in the CD34^{+}KSL fraction, which contains proliferating HSPCs during early recovery phase (Sato et al., 1999). PRC can regulate cellular proliferation by modulating *Tfam* expression (Andersson and Scarpulla, 2001), and thus the differences in

Figure 4 Mitochondrial activity and mTORC1 activation during late recovery phase. Mitochondrial activity and intracellular ROS, as measured by MDR and DCFDA staining patterns, respectively, on (Ai) day 7 and (Aii) day 9 in various fractions of WT and PGC-1$\alpha^{-/-}$ BM cells (n = 3). (Aiii) Proportion of early fractions of BM cells with high (MitoTracker^{+}DCFDA^{high}) and low (MitoTracker^{+}DCFDA^{dim}) mitochondrial activities is shown (n = 3–4 per group, *$p < 0.05$ compared to WT mice and **$p < 0.05$ compared to day7). Representative dot plots of JC-1 staining pattern as a measure of $\Delta\psi_m$ of various sub-populations of BM cells on (Bi) day 7 and (Bii) day 9 are shown. Percentage of IL-7R^{-}KL and of IL-7R^{-}KSL cells with actively respiring mitochondria (expressing JC-1 aggregate) on (Ci) day 7 and (Ciii) day 9 and (Cii) $\Delta\psi_m$ on day 7 based on JC-1$_{aggregate}$ mean fluorescence intensity (MFI) is shown (n = 3–5, *$p < 0.05$ compared to WT mice). (D) pS6 on day 7 in WT and PGC-1$\alpha^{-/-}$ BM cells are shown. (E) Representative plot showing size of WT and PGC-1$\alpha^{-/-}$ IL-7R^{-}KL and IL-7R^{-}KSL cells on day 7 post-5-FU challenge as measured by flow cytometry is shown (n = 3).

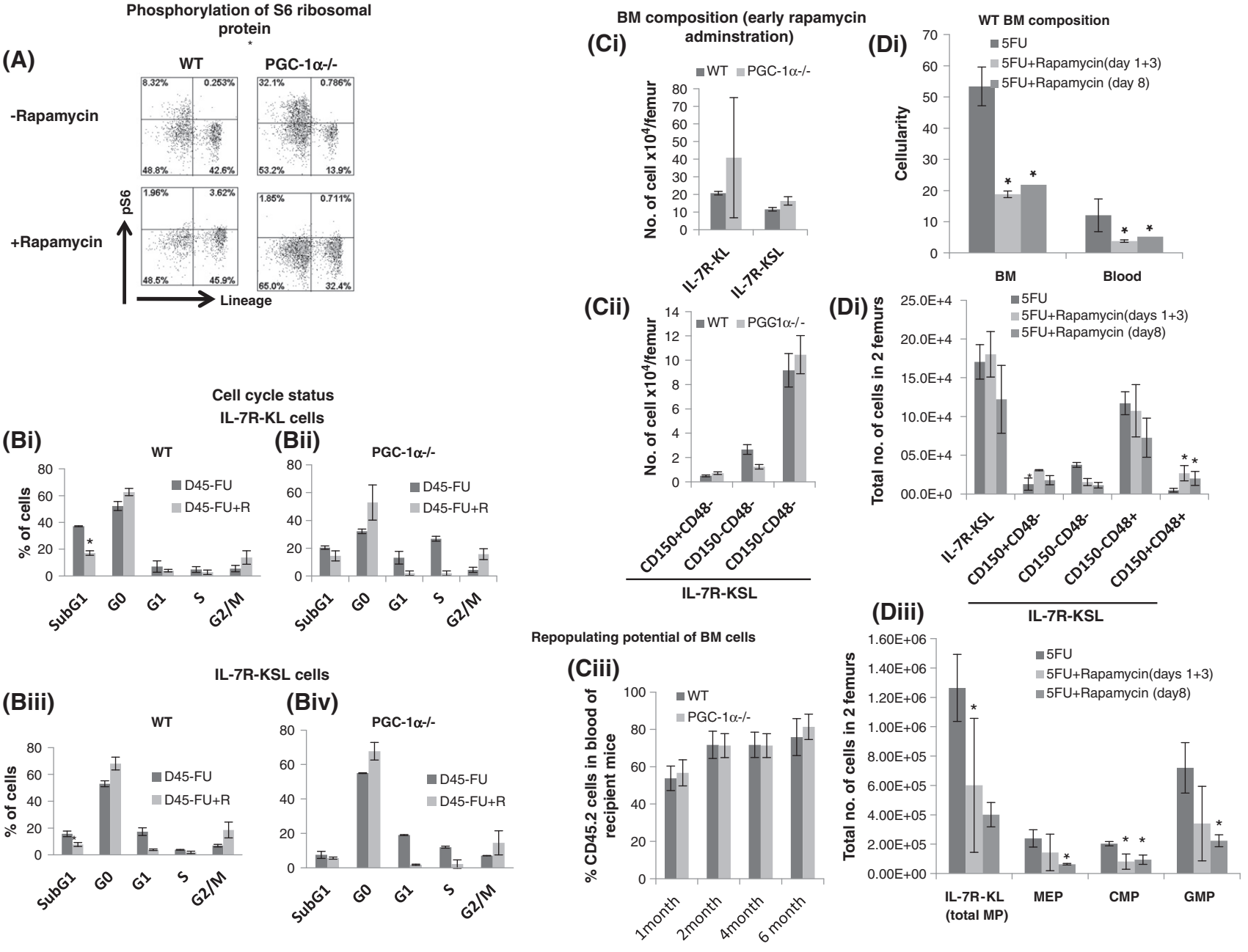
Phosphorylation of S6 ribosomal protein
(A)
WT
PGC-1α-/-
-Rapamycin
+Rapamycin
8.32%
0.253%
48.8%
42.6%
32.1%
0.786%
53.2%
13.9%
1.96%
3.62%
48.5%
45.9%
1.85%
0.711%
65.0%
32.4%
pS6
Lineage
BM composition (early rapamycin adminstration)
(Ci)
WT
PGC-1α-/-
No. of cell x10^4/femur
IL-7R-KL
IL-7R-KSL
(Cii)
WT
PGC1α-/-
No. of cell x10^4/femur
CD150+CD48-
CD150-CD48-
CD150-CD48-
IL-7R-KSL
WT BM composition
(Di)
5FU
5FU+Rapamycin(day 1+3)
5FU+Rapamycin (day 8)
Cellularity
BM
Blood
(Di)
5FU
5FU+Rapamycin(days 1+3)
5FU+Rapamycin (day8)
Total no. of cells in 2 femurs
IL-7R-KSL
CD150+CD48-
CD150-CD48-
CD150-CD48+
CD150+CD48+
IL-7R-KSL
Cell cycle status
IL-7R-KL cells
(Bi)
WT
(Bii)
PGC-1α-/-
D45-FU
D45-FU+R
% of cells
SubG1
G0
G1
S
G2/M
IL-7R-KSL cells
(Biii)
WT
(Biv)
PGC-1α-/-
Repopulating potential of BM cells
(Ciii)
WT
PGC-1α-/-
% CD45.2 cells in blood of recipient mice
1month
2month
4month
6 month
(Diii)
IL-7R-KSL
5FU
5FU+Rapamycin(days 1+3)
5FU+Rapamycin (day8)
Total no. of cells in 2 femurs
IL-7R-KL (total MP)
MEP
CMP
GMP

PRC expression could explain the differences in *Tfam* expression between PGC-1$\alpha^{-/-}$ and WT BM sub-populations observed during early recovery phase.

Late phase of hematopoietic recovery

Unlike day 4, on day 7, detectable levels of *PRC* as well as *PGC-1*α/β were expressed in both WT HSCs and MPs. PGC-1β expression level on day 7 was comparable to the basal level while PGC-1α expression in WT MPs was significantly higher than the basal level (Fig. 3Fi–v).

Coinciding with the higher expression of various PGC-1 family members on day 7 in WT HSPCs, particularly PGC-1α expression, proportion of MPs and IL-7R$^-$KSL cells undergoing mitochondrial metabolism was also higher in WT than PGC-1$\alpha^{-/-}$ mice (Figs. 4Ai, Bi, Ci–ii); this was more pronounced on day 9 (Figs. 4Aii, Bii, Ciii). Moreover, greater proportion of cells were expressing JC-1_{agg} and intracellular ROS, and ATP levels were also higher in WT cells suggesting higher mitochondrial metabolism in these cells (Figs. 4Ai–iii, 3Ei).

Unlike day 4 when mTORC1 activation was higher in PGC-1$\alpha^{-/-}$ HSPCs, on day 7 mTORC1 activation was higher in WT HSPCs (Fig. 4D). Consistent with this finding, the mean size of WT MPs and IL-7R$^-$KSL cells during the later recovery phase was also relatively bigger than corresponding PGC-1$\alpha^{-/-}$ BM cells (Fig. 4E).

Differential expression of REDD1 in WT and PGC-1$\alpha^{-/-}$ mice following 5-FU treatment

Interestingly, mTORC1 activation was higher in WT compared to PGC-1$\alpha^{-/-}$ BM cells when the cells were stimulated with growth factors in vitro (Fig. 5Ai–ii), as demonstrated by pS6 level. This finding was inconsistent with mTORC1 levels observed in HSPCs during early recovery phase but was similar to that observed during later recovery phase (Fig. 4D). mTORC1 activation is regulated by different pathways, including PI3K/Akt and REDD1 (Hay and Sonenberg, 2004; Brugarolas et al., 2004). Activated Akt levels were comparable in WT and PGC-1$\alpha^{-/-}$ HSPCs following 5-FU treatment (Fig. S5). Thus, the difference in pS6 levels between WT and PGC-1$\alpha^{-/-}$ HSPCs on day 4 was not due to differences in Akt activation. Next, I examined *REDD1* expression in these cells at steady-state and following 5-FU treatment. *REDD1* expression is regulated by ROS (Ellisen et al., 2002), and *REDD1* impairs mTORC1 activation (Sofer et al., 2005). Compared to basal level (Fig. S7B), expression of *REDD1* was higher on day 4 in both WT and PGC-1$\alpha^{-/-}$ HSPCs (Fig. 5Bi–ii); moreover, relative expression of *REDD1* on day 4 was higher in WT compared to PGC-1$\alpha^{-/-}$ HSPCs. In contrast, on day 7, *REDD1* levels decreased in both WT and PGC-1$\alpha^{-/-}$ HSPCs, coinciding with higher expression of the genes regulating mitochondrial biogenesis and respiratory chain capacity of mitochondria (Fig. 5Bi–ii). However, relative *REDD1* expression on day 7 was higher in PGC-1$\alpha^{-/-}$ than WT HSPCs (Fig. 5Biii–iv).

Effect of rapamycin treatment on HSC and MP expansion following 5-FU challenge

As shown earlier, mTORC1 is activated in HSPCs following 5-FU treatment (Figs. 3A & 4D). mTORC1 activation leads to increased demand for ATP, and an increase in ADP/ATP ratio in cell leads to activation of AMP Kinase (AMPK) (Hardie et al., 1998; Habib, 2011). Indeed AMPK activity was higher on day 4 compared to day 1 in lineage negative fraction of both WT and PGC-1$\alpha^{-/-}$ BM cells (Fig. S8) as indicated by higher phosphorylation levels AMPK (Thr172) and of ACC(Ser79) (Munday, 2002). Furthermore, analysis of phospho-p53 blot showed that, on day 4 while p53 was undergoing degradation in PGC-1$\alpha^{-/-}$ cells, it was relatively stable in WT cells; however on day 7, p53 was degraded in both WT and PGC-1$\alpha^{-/-}$ cells. Expression of PGC-1 family members, except PRC, decreases in HSPCs following 5-FU treatment; this finding suggests that the ability of HSPCs to boost electron transport chain (ETC) capacity during initial recovery phase is decreased. Therefore, it would be expected that lowering mTORC1 activation during early recovery phase would lower energy demand in HSCs and thus decrease the load on ETC, leading to lower apoptosis and improved HSC numbers. Indeed, treatment with rapamycin, an inhibitor of TORC1 pathway, on alternate days (first dose on day 1 and the second dose administered on day 3) following 5-FU, did not have any significant effect on phosphorylation level of p90RSK but decreased phosphorylated levels of both p70S6k and S6 ribosomal (Figs. S5 & 6A) and lowered apoptosis (Fig. 6Bi–iv) in WT and PGC-1$\alpha^{-/-}$ MPs and IL-7R$^-$KSL cells. Consistent with lowering of mTORC1 activation, cell sizes of WT and PGC-1$\alpha^{-/-}$ MPs and IL-7R$^-$KSL cells were comparable (Fig. S9A). Also, mitochondrial mass and activity and ROS levels of WT and PGC-1$\alpha^{-/-}$ MPs and IL-7R$^-$KSL cells were also comparable (Figs. S9B–D, Ei–iii).

Figure 6 Effect of rapamycin on HSC and progenitor cell pools following 5-FU challenge. (A) pS6 levels on day 4 post 5-FU challenge in the BM cells of WT and PGC-1$\alpha^{-/-}$ mice, which had been either treated with rapamycin on days 1 and 3 post 5-FU injection or left untreated, are shown. Representative plot shown (n = 3). (B) Effect of rapamycin treatment on cell cycle status of MPs (IL-7R$^-$KL) of (Bi) WT and (Bii) PGC-1$\alpha^{-/-}$, and IL-7R$^-$KSL cells of (Biii) WT and (Biv) PGC-1$\alpha^{-/-}$ cells on day 4 following 5-FU treatment alone or along with rapamycin treatment as described above (n = 3, *$p < 0.05$ compared to no rapamycin treatment of same genotype). (Ci) Total number of MPs and IL-7R$^-$KSL cells and (Cii) HSCs identified using SLAM markers in WT and PGC-1$\alpha^{-/-}$ mice on day 6 post-5-FU is shown (n = 3). (Ciii) Competitive repopulating potential of 5-FU treated BM cells of WT or PGC-1$\alpha^{-/-}$ mice on day 6 post-5-FU treatment and that of untreated WT mice is shown. 2×10^5 BM cells (CD45.2) were mixed with competitor cells from BoyJ mice (CD45.1) and injected into lethally irradiated F1 (CD45.1/CD45.2) mice at 1: donor:competitor cell ratio. Data shows mean (±SD) contribution of donor-derived cells in the peripheral blood of recipient mice at various time after transplantation (*$p < 0.05$, n = 5). (Di) Total BM cellularity ($\times 10^6$ for 2 femurs) and PBC count ($\times 10^6$/ml) on day 12 of WT mice treated with 5-FU alone or 5-FU followed by rapamycin treatment on days 1 and 3 or 5-FU followed by rapamycin treatment on day 8. Effect of above-mentioned treatments on (Dii) HSCs and (Diii) total and sub-sets of MPs are shown (*$p < 0.05$, n = 3).

OXPHOS is the major source of cellular NADH and, therefore endogenous NADH level is an indicator of mitochondrial metabolism (Simsek et al., 2010; Chance and Thorell, 1959). Moreover, antimycin A, an inhibitor of complex III of ETC, leads to a buildup of NADH in cells undergoing mitochondrial metabolism. Interestingly, significantly greater proportions of both WT and PGC-1$\alpha^{-/-}$ IL-7R^{-}KSL cells were undergoing mitochondrial metabolism on day 4 post-5-FU than untreated cells as indicated by NADH fluorescence pattern and an increase in proportion of cells expressing NADH upon treatment with antimycin A (Fig. S9Fi). Importantly, the amount of NADH per cell was also high on day 4 post-5-FU treatment as demonstrated by MFI of NADH fluorescence (Fig. S9Fi–ii). However, NADH fluorescence intensity and pattern were comparable between WT and PGC-1$\alpha^{-/-}$ HSPCs on day 4 post-5-FU challenge when the mice were treated with rapamycin (Fig. S9Fiv) unlike that observed in the absence of rapamycin treatment (Fig. 3Diii). Concomitantly with changes with lower mTORC1 activation and mitochondrial activity, the proportion of both WT and PGC-1$\alpha^{-/-}$ HSPCs undergoing proliferation was also reduced (Fig. 6Bi–iv). In addition, this regimen of rapamycin treatment did not have any significant effect on the total number of early sub-populations of WT BM cells on day 4 post-5-FU treatment, but it significantly reduced total HSC and MP numbers and altered mature cell composition in BM of PGC-1$\alpha^{-/-}$ mice (Figs. S10A, B & D). However, on day 7, the effect of rapamycin treatment on WT hematopoietic recovery was pronounced—rapamycin led to higher PBC count, BM cellularity, MPs and HSCs (Figs. S10Bi–iv & C). The inhibitory effect of rapamycin on PGC-1$\alpha^{-/-}$ HSPC numbers is consistent with the finding that in PGC-1$\alpha^{-/-}$ mice, higher mTORC1 activation along with higher mitochondrial capacity during early recovery phase that supports enhanced proliferative potential is the major contributing factor for increased HSPC pool in PGC-1$\alpha^{-/-}$ mice. Rapamycin treatment initiated early following 5-FU challenge resulted in recovery of comparable numbers of MPs, MPPs and HSCs on day 6 in WT and PGC-1$\alpha^{-/-}$ mice (Fig. 6Ci–ii) and also led to comparable competitive reconstituting ability of WT and PGC-1$\alpha^{-/-}$ BM cells (Fig. 6Ciii), unlike the differences in repopulating activity of WT and PGC-1$\alpha^{-/-}$ BM cells treated with 5-FU alone. Rapamycin treatment also led to early recovery of blood cells in WT mice (Fig. S10Cii) although it subdued the overshoot of blood cell production that occurs during late recovery phase (Fig. 6Di).

Treatment of mice with a single dose of rapamycin on day 8 post-5-FU injection significantly reduced MPs, total BM cellularity and PBC counts (Fig. 6Di–iii). Moreover, reduction in MPs (particularly GMP and MEP) was higher when rapamycin was administered on day 8 compared to early rapamycin administration (on days 1 and 3) (Fig. 6Ciii). However, the pronounced effect of rapamycin on WT HSC numbers when administered during the early recovery phase was not reproduced with rapamycin administration on day 8 (Fig. 6Cii). HSCs rapidly proliferate during days 2–5 post-5-FU challenge, and, thereafter, their proliferation slows down (Lerner and Harrison, 1990; Hodgson and Bradley, 1979). The current data show that the HSCs have limited ability to boost mitochondrial biogenesis during early phase, and, thus, suppression of mTORC1 activation by rapamycin treatment during this phase would alleviate the energy stress and thus preserve the HSCs. Thus, the differential effect of rapamycin on WT HSC numbers based on its administration schedule post-5-FU treatment is consistent with these findings.

PGC-1α is also expressed by adipocytes in addition to HSPCs(Puigserver and Spiegelman, 2003). Since adipocytes are a type of stromal cell and influence hematopoiesis (Greenberger, 1978), I next investigated whether the differences between WT and PGC-1$\alpha^{-/-}$ HSCs observed during early hematopoietic recovery phase were hematopoietic cell intrinsic. To address this issue, recovery of hematopoiesis following 5-FU challenge was analyzed in chimeric mice. The chimeric mice were generated by reconstituting hematopoiesis in lethally irradiated BoyJ mice with BM cells from 5-FU treated WT or PGC-1$\alpha^{-/-}$ mice. Although HSC numbers after 5-FU treatment are different in WT and PGC-1$\alpha^{-/-}$, rapamycin treatment on days 1 and 3 post-5-FU challenge leads to comparable numbers of HSCs in BM of WT and PGC-1$\alpha^{-/-}$ mice following 5-FU treatment. Therefore, to inject comparable numbers of HSCs, lethally irradiated BoyJ mice (CD45.1) were transplanted with 2×10^5 BM cells from 6d 5-FU treated WT or PGC-1$\alpha^{-/-}$ mice that received rapamycin treatment on days 1 and 3 post-5-FU challenge. At 7 months post-transplantation, the chimeric mice had comparable levels of donor derived blood cell in circulation (>97%) irrespective of whether they received WT (WT/Boy/J chimeric) BM cells or PGC-1$\alpha^{-/-}$ (PGC-1$\alpha^{-/-}$/Boy/J chimeric) BM cells. Moreover, both the BM and blood cellularity were also comparable (Fig. S9Ai). Similarly, the contribution of donor derived MPs and HSC enriched fractions (IL-7R^{-}KSL) of cells in the BM of chimeric mice were comparable (Fig. S11Aii–iii). However, upon 5-FU treatment, BM cellularity, donor derived HSCs, and MPs on day 5 were higher in PGC-1$\alpha^{-/-}$/BoyJ chimeric mice than WT/BoyJ chimeric mice (Fig. S11Bi–iii). Furthermore, on day 5, similar to PGC-1$\alpha^{-/-}$ mice, PGC-1$\alpha^{-/-}$/BoyJ chimeric mice also had higher proportion of cells that were in cell cycle compared to WT/BoyJ mice (Fig. S11C). Moreover, expression of *PRC*, *Tfam* genes was higher and *REDD-1* gene lower in CD45.2 Lin^{-} BM cells isolated from PGC-1$\alpha^{-/-}$/BoyJ chimeric mice compared to corresponding cells isolated from WT/BoyJ chimeric mice (Fig. S10D). These findings, thus, establish that the differences in HSCs between WT and PGC-1$\alpha^{-/-}$ mice during early recovery phase following 5-FU challenge are indeed hematopoietic cell intrinsic.

Discussion

HSCs are relatively quiescent and proliferate slowly at steady-state; obliteration of hematopoietic progenitors by 5-FU forces a majority of HSCs to undergo proliferation to rescue hematopoiesis. Therefore, understanding recovery of hematopoiesis following 5-FU treatment is an ideal model to gain insight into the molecular mechanisms that regulate HSC expansion in vivo. Growth factors responsible for driving HSPC proliferation are elevated soon after 5-FU treatment (Rich, 1991), however, the recovery of hematopoiesis following 5-FU treatment appears to occur in two phases. First, HSCs undergo rapid proliferation, and this is followed by the second phase during which progenitor cells undergo proliferation, leading to replenishment of mature hematopoietic cells in the BM and recovery of PBC count. The current findings demonstrate that expression of PGC-1

family members in HSPCs differs during these two phases of hematopoietic recovery. At steady-state, WT HSPCs express all three known PGC-1 family members, but, during early phase of hematopoietic recovery, only PRC is expressed in HSPCs. During the later phase, expression of all the three members of PGC-1 family reappears in HSPCs. Furthermore, PRC plays an important role during the initial recovery phase, while PGC-1α plays critical role in the later recovery phase. mTORC1 activation, which drives HSPCs' proliferation, creates increased demand for energy in HSPCs, and the current findings show that both mTORC1 activation level and recovery of hematopoiesis following 5-FU are modulated by the mitochondrial activity of HSPCs.

During steady-state hematopoiesis, although HSCs are mostly quiescent and undergo chiefly glycolytic metabolism (Simsek et al., 2010; Takubo et al., 2010), they express all known members of the PGC-1 family (Basu et al., 2013). However, mitochondrial metabolism is limited in HSCs during steady-state, probably due to restricted availability of O_2 in endosteal niche and high HIF-1α expression in these cells (Simsek et al., 2010; Takubo et al., 2010). Also, severely restricting dependence on mitochondrial metabolism derived energy is critical for maintenance of HSCs at steady-state as activation of mitochondrial metabolism due to loss of autophagy gene Atg7 causes depletion of HSCs (Mortensen et al., 2011). Interestingly, on day 4 post-5-FU challenge, both PGC-1α/β expressions were undetectable in HSPCs. 5-FU treatment leads to collapse of sinusoids in the bone marrow and the killing of hematopoietic progenitor cells (Heissig et al., 2002). Thus, availability of 'oxygen pockets' in the BM post-5-FU treatment is likely to be lower than in unperturbed BM. In addition to mitochondrial ETC capacity, availability of sufficient O_2 is required during OXPHOS to minimize the generation of superoxide and thus oxidative stress. As 5-FU treatment leads to diminution of relatively O_2-rich regions in the BM, following very high mitochondrial activity under these conditions would increase oxidative stress in and cause loss of HSCs, which may explain why expression of mitochondrial biogenesis genes is transiently low in HSPCs post-5-FU treatment. The mechanism of regulation of PGC-1 co-activators' expression in HSCs following 5-FU related and other stress hematopoiesis is a subject for further future study.

The second phase of hematopoietic recovery coincides with the reappearance of expression of all members of PGC-1 coactivators in WT HSPCs, enabling WT MPs to increase mitochondrial biogenesis and metabolism. Interestingly, although expression of all members of PGC-1 co-activators in WT progenitors was elevated during the late recovery phase, expression in HSCs was comparable to that of basal level. The late phase of recovery is characterized by slowing HSC proliferation (Harrison and Lerner, 1991; Randall and Weissman, 1997) and rapid increase in progenitor cell proliferation, leading to generation of sufficient numbers of blood cells. Unlike in WT mice, expansion of MPs during late recovery phase is impaired in PGC-1$\alpha^{-/-}$ mice (Fig. 3Bi). Proliferation of PGC-1$\alpha^{-/-}$ HSCs also slows during the second phase of recovery. However, the compounded loss of PGC-1α and lower expression of PRC likely impair cells' ability to generate sufficient mitochondrial dependent energy leading to lower HSC number (Hao et al., 2010).

HSCs are sensitive to ROS; excessive ROS level following mTOR activation has been reported to be the underlying cause of HSC loss (Chen et al., 2008), although not always (Lee et al., 2010). Since OXPHOS is a major source of cellular ROS, it is likely that activation of mTOR in HSCs is modulated to prevent significant buildup of ROS in HSCs. In support of this argument, I found that the expression of *REDD1*, a crucial inhibitor of mTOR activation (Brugarolas et al., 2004; Reiling and Hafen, 2004), in HSCs correlated with mitochondrial ETC of HSCs. Interestingly, the findings of the current study show that relatively higher apoptosis in WT HSCs was not due to the higher level of ROS in these cells, as NAC treatment initiated soon after 5-FU challenge did not improve HSC numbers in WT mice (data not shown). Rather, higher apoptosis of WT HSPCs during early recovery phase was due to lower mitochondrial ETC capacity, and increased mTOR activation. Although HSCs at steady-state mainly undergo glycolytic metabolism (Simsek et al., 2010; Takubo et al., 2010), findings of the current study demonstrate that expansion of HSCs following 5-FU treatment is dependent on mitochondrial metabolism. The critical role of mitochondria in HSCs' maintenance is further supported by the findings that deficiency of Lkb1 leads to HSC depletion (Nakada et al., 2010; Gurumurthy et al., 2010). Depletion of HSCs in Lkb1 deficient mice is associated with mitochondrial dysfunction and energy production (Gan et al., 2010). Furthermore, I found lowering mTOR activation during early phase by rapamycin treatment preserved WT HSCs and led to their improved numbers during later stage, likely by reducing energy stress. Energy stress can lead to p53 activation resulting in senescence (Lee et al., 2010) or apoptosis or reduction in the ability to undergo symmetric division—critical for stem cell expansion, as seen in mammary stem cells (Cicalese et al., 2009).

The findings of this study show that mTORC1 activation can lead to increased HSC proliferation provided the HSCs have the capacity to boost ETC to meet the increased demand for energy created by mTORC1 activation. An earlier study had shown that mTOR activation leads to the loss of HSCs due to increased mitochondrial metabolism (Chen et al., 2008). Although the current findings appear to contradict the finding of the previous study (Chen et al., 2008), differences in hematopoiesis models—stress versus steady-state—analyzed may account for the difference. Unlike steady-state, a majority of HSCs undergo proliferation (Harrison and Lerner, 1991) post-5-FU treatment to replenish hematopoiesis. 5-FU treatment leads to myeloablation and loss of a majority of sinusoidal microvasculature in BM (Kopp et al., 2005). It is likely that the loss of BM microvasculature severely restricts the availability of nutrients. Although ATP can be derived from glycolysis, OXPHOS yields maximum ATP molecules per molecule of glucose. It is therefore likely that post-5-FU treatment HSCs boost mitochondrial metabolism to meet the increased energy demand required to support rapid proliferation of HSCs. Indeed the difference in proportion of IL-7R-KSL cells undergoing mitochondrial metabolism post-5-FU treatment compared to that of untreated cells (as shown by NADH fluorescence pattern in the presence and absence of antimycin A) supports the conjecture and demonstrates an increase in mitochondrial metabolism in HSCs during initial recovery of hematopoietic phase following 5-FU treatment,

unlike steady-state hematopoiesis, during which glycolysis is required for the maintenance of HSCs (Simsek et al., 2010). However, if the HSCs lack the ability to enhance ETC activity in tune with increased mTORC1 activity, mTORC1 activation leads to the loss of HSCs, as observed in the case of WT mice. Thus, a fine tuning between mTORC1 activation and mitochondrial biogenesis is important for efficient expansion of HSPCs following 5-FU treatment.

In future studies, agents that enhance expression of PGC family members will be identified and exploited for improving in vitro expansion of HSPCs.

Supplementary data to this article can be found online at http://dx.doi.org/10.1016/j.scr.2013.10.006.

Acknowledgments

I thank Ms. Kimberly Stone at IUSM Flow Facility for sorting the cells. I also thank Ms Sharmila Paul for editing the manuscript.

References

Andersson, U., Scarpulla, R.C., 2001. Pgc-1-related coactivator, a novel, serum-inducible coactivator of nuclear respiratory factor 1-dependent transcription in mammalian cells. Mol. Cell. Biol. 21, 3738–3749.

Banki, K., Hutter, E., Gonchoroff, N.J., Perl, A., 1999. Elevation of mitochondrial transmembrane potential and reactive oxygen intermediate levels are early events and occur independently from activation of caspases in Fas signaling. J. Immunol. 162, 1466–1479.

Basu, S., Broxmeyer, H.E., 2005. Transforming growth factor-{beta} 1 modulates responses of $CD34^+$ cord blood cells to stromal cell-derived factor-1/CXCL12. Blood 106, 485–493.

Basu, S., Broxmeyer, H.E., Hangoc, G., 2013. Peroxisome proliferator-activated-gamma coactivator-1alpha-mediated mitochondrial biogenesis is important for hematopoietic recovery in response to stress. Stem Cells Dev. 22, 1678–1692.

Brugarolas, J., Lei, K., Hurley, R.L., et al., 2004. Regulation of mTOR function in response to hypoxia by REDD1 and the TSC1/TSC2 tumor suppressor complex. Genes Dev. 18, 2893–2904.

Chance, B., Thorell, B., 1959. Localization and kinetics of reduced pyridine nucleotide in living cells by microfluorometry. J. Biol. Chem. 234, 3044–3050.

Chen, C., Liu, Y., Liu, R., et al., 2008. TSC–mTOR maintains quiescence and function of hematopoietic stem cells by repressing mitochondrial biogenesis and reactive oxygen species. J. Exp. Med. 205, 2397–2408.

Cicalese, A., Bonizzi, G., Pasi, C.E., et al., 2009. The tumor suppressor p53 regulates polarity of self-renewing divisions in mammary stem cells. Cell 138, 1083–1095.

Cossarizza, A., Salvioli, S., 2001. Flow cytometric analysis of mitochondrial membrane potential using JC-1. Curr. Protoc. Cytom. 13, 9.14.1–9.14.7.

Dennis, P.B., Jaeschke, A., Saitoh, M., et al., 2001. Mammalian TOR: a homeostatic ATP sensor. Science 294, 1102–1105.

Ellisen, L.W., Ramsayer, K.D., Johannessen, C.M., et al., 2002. REDD1, a developmentally regulated transcriptional target of p63 and p53, links p63 to regulation of reactive oxygen species. Mol. Cell 10, 995–1005.

Fingar, D.C., Blenis, J., 2004. Target of rapamycin (TOR): an integrator of nutrient and growth factor signals and coordinator of cell growth and cell cycle progression. Oncogene 23, 3151–3171.

Gan, B., Hu, J., Jiang, S., et al., 2010. Lkb1 regulates quiescence and metabolic homeostasis of haematopoietic stem cells. Nature 468, 701–704.

Greenberger, J.S., 1978. Sensitivity of corticosteroid-dependent insulin-resistant lipogenesis in marrow preadipocytes of obese–diabetic (db/db) mice. Nature 275, 752–754.

Gurumurthy, S., Xie, S.Z., Alagesan, B., et al., 2010. The Lkb1 metabolic sensor maintains haematopoietic stem cell survival. Nature 468, 659–663.

Habib, S.L., 2011. Mechanism of activation of AMPK and upregulation of OGG1 by rapamycin in cancer cells. Oncotarget 2, 958–959.

Hao, W., Chang, C.P., Tsao, C.C., Xu, J., 2010. Oligomycin-induced bioenergetic adaptation in cancer cells with heterogeneous bioenergetic organization. J. Biol. Chem. 285, 12647–12654.

Hardie, D.G., Carling, D., Carlson, M., 1998. The AMP-activated/SNF1 protein kinase subfamily: metabolic sensors of the eukaryotic cell? Annu. Rev. Biochem. 67, 821–855.

Harrison, D.E., Lerner, C.P., 1991. Most primitive hematopoietic stem cells are stimulated to cycle rapidly after treatment with 5-fluorouracil. Blood 78, 1237–1240.

Hay, N., Sonenberg, N., 2004. Upstream and downstream of mTOR. Genes Dev. 18, 1926–1945.

Heissig, B., Hattori, K., Dias, S., et al., 2002. Recruitment of stem and progenitor cells from the bone marrow niche requires MMP-9 mediated release of kit-ligand. Cell 109, 625–637.

Hodgson, G.S., Bradley, T.R., 1979. Properties of haematopoietic stem cells surviving 5-fluorouracil treatment: evidence for a pre-CFU-S cell? Nature 281, 381–382.

Jansen, R., Damia, G., Usui, N., et al., 1991. Effects of recombinant transforming growth factor-beta 1 on hematologic recovery after treatment of mice with 5-fluorouracil. J. Immunol. 147, 3342–3347.

Kalaitzidis, D., Neel, B.G., 2008. Flow-cytometric phosphoprotein analysis reveals agonist and temporal differences in responses of murine hematopoietic stem/progenitor cells. PLoS One 3, e3776.

Kelly, D.P., Scarpulla, R.C., 2004. Transcriptional regulatory circuits controlling mitochondrial biogenesis and function. Genes Dev. 18, 357–368.

Kopp, H.G., Avecilla, S.T., Hooper, A.T., et al., 2005. Tie2 activation contributes to hemangiogenic regeneration after myelosuppression. Blood 106, 505–513.

Laplante, M., Sabatini, D.M., 2009. mTOR signaling at a glance. J. Cell Sci. 122, 3589–3594.

Larsson, N.G., Wang, J., Wilhelmsson, H., et al., 1998. Mitochondrial transcription factor A is necessary for mtDNA maintenance and embryogenesis in mice. Nat. Genet. 18, 231–236.

Lee, J.Y., Nakada, D., Yilmaz, O.H., et al., 2010. mTOR activation induces tumor suppressors that inhibit leukemogenesis and deplete hematopoietic stem cells after Pten deletion. Cell Stem Cell 7, 593–605.

Lerner, C., Harrison, D.E., 1990. 5-Fluorouracil spares hemopoietic stem cells responsible for long-term repopulation. Exp. Hematol. 18, 114–118.

Mortensen, M., Soilleux, E.J., Djordjevic, G., et al., 2011. The autophagy protein Atg7 is essential for hematopoietic stem cell maintenance. J. Exp. Med. 208, 455–467.

Munday, M.R., 2002. Regulation of mammalian acetyl-CoA carboxylase. Biochem. Soc. Trans. 30, 1059–1064.

Nakada, D., Saunders, T.L., Morrison, S.J., 2010. Lkb1 regulates cell cycle and energy metabolism in haematopoietic stem cells. Nature 468, 653–658.

Pieri, C., Recchioni, R., Moroni, F., 1993. Age-dependent modifications of mitochondrial trans-membrane potential and mass in rat splenic lymphocytes during proliferation. Mech. Ageing Dev. 70, 201–212.

Puigserver, P., Spiegelman, B.M., 2003. Peroxisome proliferator-activated receptor-gamma coactivator 1 alpha (PGC-1 alpha): transcriptional coactivator and metabolic regulator. Endocr. Rev. 24, 78–90.

Randall, T.D., Weissman, I.L., 1997. Phenotypic and functional changes induced at the clonal level in hematopoietic stem cells after 5-fluorouracil treatment. Blood 89, 3596–3606.

Reiling, J.H., Hafen, E., 2004. The hypoxia-induced paralogs Scylla and Charybdis inhibit growth by down-regulating S6K activity upstream of TSC in Drosophila. Genes Dev. 18, 2879–2892.

Rich, I.N., 1991. The effect of 5-fluorouracil on erythropoiesis. Blood 77, 1164–1170.

Sato, T., Laver, J.H., Ogawa, M., 1999. Reversible expression of CD34 by murine hematopoietic stem cells. Blood 94, 2548–2554.

Scarpulla, R.C., 2002. Transcriptional activators and coactivators in the nuclear control of mitochondrial function in mammalian cells. Gene 286, 81–89.

Scarpulla, R.C., 2008. Transcriptional paradigms in mammalian mitochondrial biogenesis and function. Physiol. Rev. 88, 611–638.

Sengupta, S., Peterson, T.R., Sabatini, D.M., 2010. Regulation of the mTOR complex 1 pathway by nutrients, growth factors, and stress. Mol. Cell 40, 310–322.

Simsek, T., Kocabas, F., Zheng, J., et al., 2010. The distinct metabolic profile of hematopoietic stem cells reflects their location in a hypoxic niche. Cell Stem Cell 7, 380–390.

Smiley, S.T., Reers, M., Mottola-Hartshorn, C., et al., 1991. Intracellular heterogeneity in mitochondrial membrane potentials revealed by a J-aggregate-forming lipophilic cation JC-1. Proc. Natl. Acad. Sci. U. S. A. 88, 3671–3675.

Sofer, A., Lei, K., Johannessen, C.M., Ellisen, L.W., 2005. Regulation of mTOR and cell growth in response to energy stress by REDD1. Mol. Cell. Biol. 25, 5834–5845.

Takubo, K., Goda, N., Yamada, W., et al., 2010. Regulation of the HIF-1alpha level is essential for hematopoietic stem cells. Cell Stem Cell 7, 391–402.

Uldry, M., Yang, W., St-Pierre, J., et al., 2006. Complementary action of the PGC-1 coactivators in mitochondrial biogenesis and brown fat differentiation. Cell Metab. 3, 333–341.

Wilson, A., Laurenti, E., Oser, G., et al., 2008. Hematopoietic stem cells reversibly switch from dormancy to self-renewal during homeostasis and repair. Cell 135, 1118–1129.

Yilmaz, O.H., Kiel, M.J., Morrison, S.J., 2006. SLAM family markers are conserved among hematopoietic stem cells from old and reconstituted mice and markedly increase their purity. Blood 107, 924–930.